Experimental investigation on ferrofluid properties of Cd doped Co-Zn ferrites

R. Manimegalai[a,*], S. Sendhilnathan[b], V. Chithambaram[c], M. Kumar[d]
[a]*Department of Physics, K.Ramakrishnan College of Engineering Trichy-621112, Tamilnadu, India*
[b]*Professor, Department of Physics, University College of Engineering, Pattukkottai Campus, Rajamadam– 614701.Tamilnadu, India*
[c]*Department of Physics, Karpaga Vinayaga College of Engineering and Technology, Chengalpattu, Tamilnadu, India 603308*
[d]*Department of Chemistry, Kings Engineering college, Chennai*

The Co-Zn ferrites $Co_{0.5}Zn_{0.5}Cd_xFe_{(2-x)}O_4$ (x-0.0, 0.1, 0.2, 0.3, 0.4, and 0.5) were synthesized by CO-precipitation method. The dielectric and structural properties has been investigated by effect of Cd doping in Co-Zn spinel ferrites. Dielectric constants were studied dependence of the frequency and temperature thus revealed that the dielectric dispersion based on the Maxwell-Wagner method polarizations are agreed with Koop's conceptualization theory. Further, dielectric properties were studies over a frequency range from 10 kHZ to 30 MHZ. The dielectric constant is varied from 2.4 to 8.4 for real parts and 0.008 to 0.42 for imaginary parts, respectively. The tangent loss also recorded as 0.003 to 0.052 at 1 MHZ due to Co ions concentrations. In high and low frequencies of grain and grain boundary contribution is an important evident for obtained dielectric constant. The obtained values of coercivity (Hc) for these ferrites range between 280.4 Oe to 1380.3 Oe, based on VSM data. By converting Zn^{2+} and Cd^{2+} to cobalt magnetic ions it is possible to convert the magnetic properties of cobalt ferrite into a potential individual for numerous technical uses. The dielectric loss at room temperature and at high frequencies is found to be quite negligible. It is also discovered that when Cd is substituted, the dielectric loss tangent reduces.

(Received February 21, 2023; Accepted April 27, 2023)

Keywords: Dielectric constant, Co-precipitation method, Spinel structure, AC and DC resistivity

1. Introduction

Ferrofluid has become a very significant research field in recent decades due to its excellent performance characteristics for various industrial applications [1]. Ferrofluids have the benefit of being able to regulate fluid heat transfer characteristics utilizing an exterior electromagnetic ground, making them useful in disciplines including electronic packaging, advanced manufacturing, temperature engineering, aviation, and biomedicine [3-5]. Often these applications include drug delivery, hypothermia, sensors, Magnetic resonance imaging (MRI) and bio imaging are based on the unique nature of magnetic particles such as super magnetism, spin canting and spin glass behaviour[6-9]. Ferrofluids are very widely used in heat management applications because the external magnetic field effectively controls the instantaneous convective heat transfer. Nevertheless, ferrohydrodynamics convection and convection heat transfer analysis are not often classified. Among the spinel ferrites Cu, Ni, Co, Mn and Zn are shows the excellent magnetic, electrical and structural properties and has been used in different field such as information storage system, printed circuit devices, energy storage device and catalysts [10-12].

Rohilla et al. successfully synthesized the $CoFe_2O_4$ and considerably ensured that the chemical flexibility, adequate saturation magnetization, multi-axial anisotropic effect and high Curie temperature [13]. Cobalt ferrite nanoparticles are an excellent choice for DNA isolation and purification, as well as

*Corresponding author: manimegalaiparthiban@gmail.com
https://doi.org/10.15251/DJNB.2023.182.547

medical applications such as polymerase chain reaction (PCR) -based DNA and hyperthermia treatment interventions [14]. Ghasemian et al prepared the $Co_{0.5}Zn_{0.5}Fe_2O_4$ magnetic particles made of cobalt zinc ferrite have been used to improve the resolution of magnetic resonance imaging (MRI) [15]. Rahimi et al. used a sol-gel auto-combustion process to successfully synthesize PVA decorated $Ni_{0.3}Zn_{0.7}Fe_2O_4$ nanomaterials, with predicted lattice parameter and magnetizations in the effective range of 17–24 nm and 16–19 emu/g, accordingly [16]. Munjal et al. used a hydrothermal approach to make oleic acid-coated water-dispersible $CoFe_2O_4$ nanomaterials exhibiting better hydrodynamic durability, and they investigated their applicability as in biomedical field [17]. Raut et al calculated the Zn substituted particle size of $CoFe_2O_4$ nano particle size increased from 45 to 49 nm by using sol-gel auto combustion method [18]. When Zn, Cd, Ni and other metal ions are topped in a cobalt ferrite structure, it changes from reverse spinel to conventional spinel ferrite [19]. Due to the addition of Zn^{2+} in Co ferrite diminish the hardness due to the hard and soft magnetic materials. $Co_xZn_{1-x}Fe_2O_4$ (zinc substituted cobalt ferrites) is a soft magnetic material along with strong chemical stability, great temperature sensitivity and high coercivity [20]. However, Co ferrites are normally used for saturation magnetization and high coercivity, but introducing the Zn ferrites changes the magnetic properties from super magnetic to ferromagnetic with low loss of energy. Co-Zn ferrites in aggregate crystalline structure synthesized using traditional ceramic techniques. There have been numerous morphological and electromagnetic analyses of nickel treated cobalt zinc ferrite nanoparticles [23], as well as morphological investigations of cadmium filled Co-Zn ferrites [24]. The sol–gel auto-combustion method was used to fabricate the Mn reinforced $Co_{0.6}Zn_{0.4}Mn_xFe_{2x}O_4$ ferrites for to analyze the catalytic degradation of electrical and magnetic properties.

Cobalt ferrite is an important material due to its high chemical stability, good mechanical hardness and high binding at nanoscale ferrites and hard magnetic properties compared to all ferrites. The magnetic characteristics of cobalt ferrite are altered when the diamagnetic ions Zn and Cd are doped in $CoFe_2O_4$. Because cobalt ferrite is ferrimagnetic under 790 K, magnetic couplings are quite powerful within that ferrite. However, the Zn^{2+} ions settled with tetrahedral sites and Fe^{3+} attributed to the octahedral sites when Co^{2+} ion replaced by Zn^{2+} $COFe_2O_4$ ferrites. In this research article synthesized the cadmium $Co_{0.5}Zn_{0.5}Cd_xFe_{(2-x)}O_4$ Cobalt ferrites by using Co-precipitation method. Because Zn possesses high resistivity, low hysteresis, excellent tensile hardness, high Thermal durability, and chemical inertness, cobalt zinc ferrite is one of the most potential soft ferrites being used electrical devices such as power transformers, steam turbines, and machines. In addition, Co-Zn combined ferrites were chosen for this study because to their high magnetic sensitivity, which is required in the above applications.

2. Materials and methods

2.1. Co-Zn ferrites synthesis method

Co-precipitation method were used to prepare the $Co_{0.5}Zn_{0.5}Cd_xFe_{(2-x)}O_4$ (x-0.0, 0.1, 0.2, 0.3, 0.4, and 0.5) Co-Zn Ferrites. As per the Stoichiometric amount of analytic materials Co $(NO_3)_2.6H_2O$ (99% purity), Zn $(NO_3)_2.6H_2O$ (98% purity), and Fe $(NO_3)_3.9H_2O$ (99% purity), and Cd $(NO_3)_2.4H_2O$ were dissolved in 100ml distilled water. Further 30 M NH4OH is added to the solution with the metal nitrate and solidified by constant stirring at 80^0 C. The temperature of the reaction was kept at 800°C for 3 hours and then cooled in the aggregate when it reached the aqueous condition. Fig 1 shows the co-precipitation procedure to synthesis the Co-Zn Ferrites with proposed proportions.

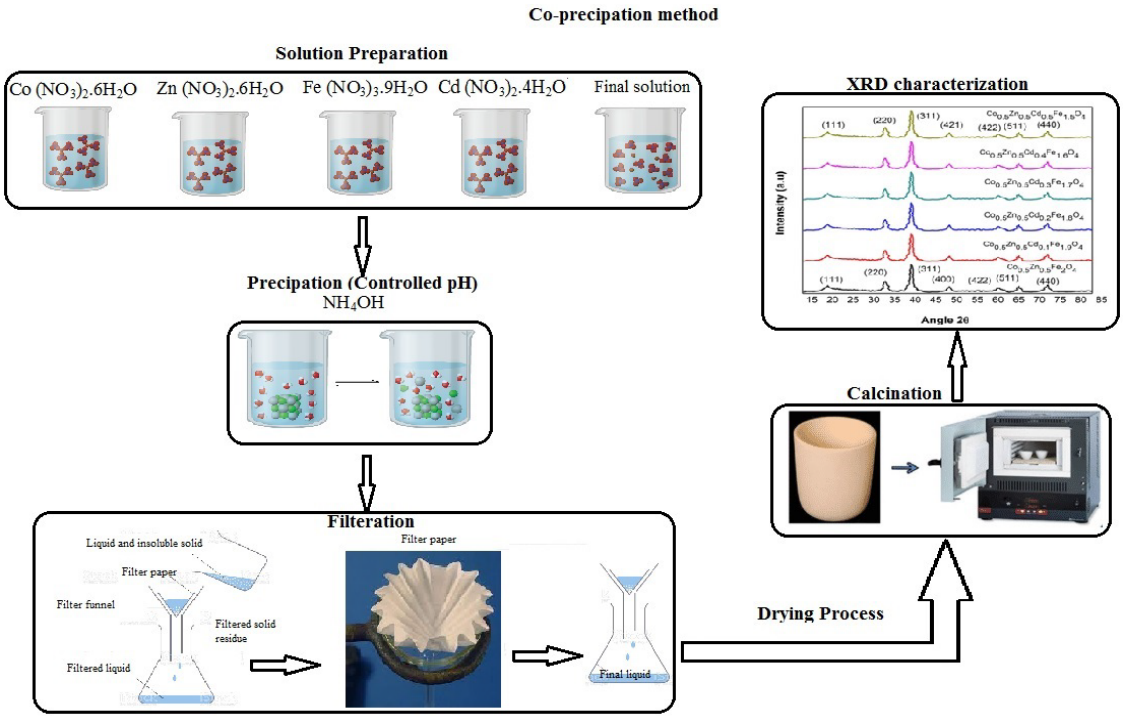

Fig. 1 Co-Zn synthesis.

3. Results and discussion

3.1. Dielectric properties

The nature of electric energy particles and the conduction process in ferrite nanoparticles are revealed by studying dielectric characteristics. The Co-Zn prepared ferrites of dielectric constant properties were estimated by the following expression

$$\varepsilon_r = \frac{C_o d}{\varepsilon_o A}$$

C_o-Capacitance, d and A are the pellet thickness, respectively and ε_o-permittivity of free face.

The ac conductivity was estimated by based on the dielectric constant and dielectric loss

The ac conductivity equation can be expressed as follows

$$\sigma_{ac} = \omega \varepsilon_0 \varepsilon' \tan \delta_\varepsilon$$

σ_{ac}-ac conductivity, and $\tan \delta_\varepsilon$ –dielectric tangent and ω-angular frequency

Debye expressed the following relaxation time during the time of dielectric dispersion.

$$\varepsilon^*(\omega) = \varepsilon'(\omega) + i\varepsilon''(\omega) = \varepsilon_\infty + \frac{\varepsilon_s}{1 + i\omega\tau}$$

ε_s, ε_∞-low and high frequency of ε'

The modified Debye equation as follows

$$\varepsilon^*(\omega) = \varepsilon'(\omega) + i\varepsilon''(\omega) = \varepsilon_\infty + \frac{\varepsilon_s}{1 + (i\omega\tau)^\alpha}$$

α lies between 0 to 1 (width parameter)

The frequency range 10 kHZ to 20 MHz of dielectric constant and tangent loss were studied at room temperature. Fig 2 and 3 shows the real and imaginary part of dielectric constant of prepared ferrites. Due to low frequency dielectric constant decreases significantly, while it decreases less in the high frequency zone. The figure depending on the Maxwell-Wagner model and Koop's theory exhibits almost frequencies broad changes in the extremely wide bandwidth range. In ferrite nanoparticles, the particles have a higher conductivity than the grain boundaries according to this paradigm and some of the conductive materials include grains isolated by the conductive grain boundaries. Further, ferrites of dipolar, and interfacial, electronic and ionic are classified as different types of polarization. At low frequency polarization are dipole polarization and interface polarization and it is essential for the conductivity constant, whereas electronic and ion polarization play a role in long wavelengths.

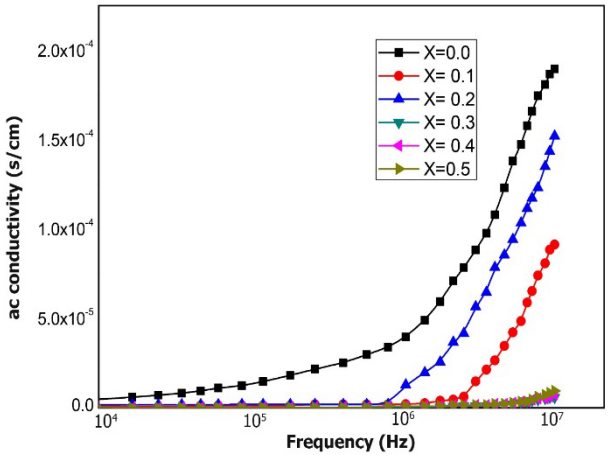

Fig. 2. Ac conductivity variations.

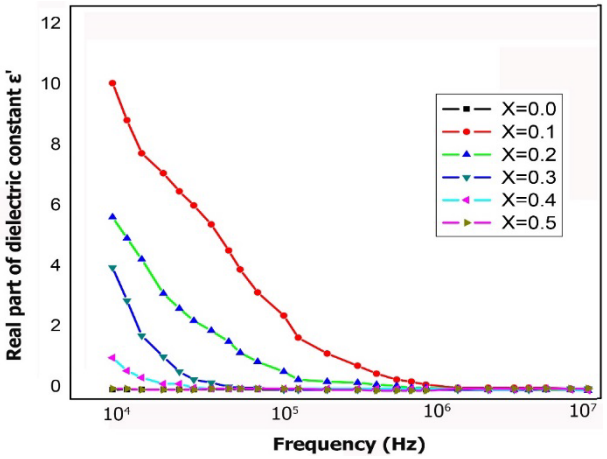

Fig. 3. Varied frequency of dielectric constant for Real part.

Depending on the charge bearer anticipating among Fe $^{2+}\leftrightarrow$ Fe^{3+}, $Co^{2}+\leftrightarrow Co_{3}+$, $Zn^{2+}\leftrightarrow Zn^{3+}$ and $Cd^{2+}\leftrightarrow Cd^{3+}$ expressed the maximum value of dielectric constant, so that electric dipoles connected with alternating field. The B-sites are occupied by inverse spinel structure Co^{2+}, Zn^{2+}, and Fe^{3+} ions in Co-Zn ferrites, while left of the part occupied by A sites. The p-type and n-type carriers are produced by Co^{2+}, Zn^{2+}, and Fe^{2+}, Fe^{3+} respectively. Therefore the electrons are only presented a carrier in A-site, while holes and electrons both identified by maximum number of frequencies. Because the hopping of electrons could indeed replicate the exterior switching force over a particular frequency, polarisation reduces and achieves a steady state as the frequency rises. As result increases frequency leads to

decreases the polarization obtain a constant value due to few frequencies of do not possess the external magnetic field. The polarizations diminish rapidly due to more time consumption than polarization mechanism and obtain the constant value by the contribution of interfacial polarizations.

Fig 4 illustrates the imaginary part of dielectric constant by varying frequencies. This is consistent with previous findings of dielectric scattering in the observed experiment. The particles in the grain accumulate at the grain boundary space over a period of time due to the maximum resistance of this grain boundary. This buildup of electrons results in the formation of the charge density and, as a result of the polarization. Even as temperature increases, additional electrons congregate at the bulk material, increasing overall polarisation and the dielectric strength. However, taking less time to sort during frequency increases the electrons, while the electrons do not follow the AC field, resulting in a lower conductivity constant.

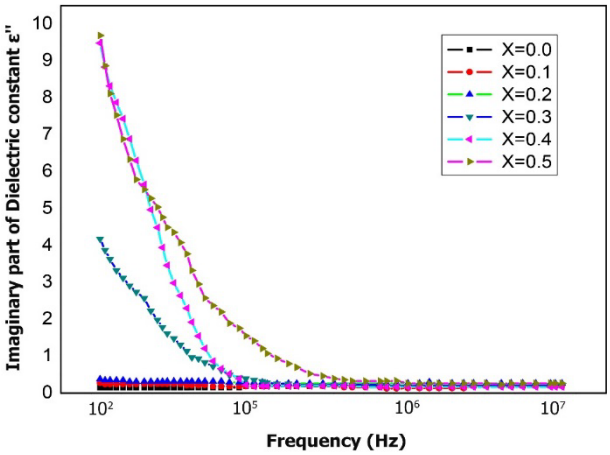

Fig. 4. Imaginary part of dielectric constant.

3.2. Tangent loss

Dielectric tangent loss was estimated by following relation

$$\tan \delta_\varepsilon = \frac{\varepsilon''}{\varepsilon'}$$

ε'- Real part, ε''-imaginary part.

Figure 4 shows the tangent loss based on the temperature difference for CZMO by different Cd doping concentrations. It is observed that $\tan \delta_\varepsilon$ loss consequently increases with temperature. The thermal relaxation processes have been observed when the increases of frequency leads to the maximum shifted towards the high temperature. The $\omega \tau = 1$ is maximum dielectric loss of ferrites (where $\omega = 2\mu f$). The jumping probability per time P desired the maximum value of τ.

$$\tau = \frac{1}{2p}$$

The fact that the peak position is change to a higher temperature as the frequency rises means that the chance of jumping the probability raises. The conductivity and tangent loss is expressed by following

$$\tan \delta = \frac{\sigma}{2\pi f \varepsilon_0 \varepsilon'}$$

The dielectric tangent loss is always proportional to the ac conductivity. As the effect of temperature rises due to the scope of the carriers produce earlier, thus accumulating the conductivity and loss tangent.

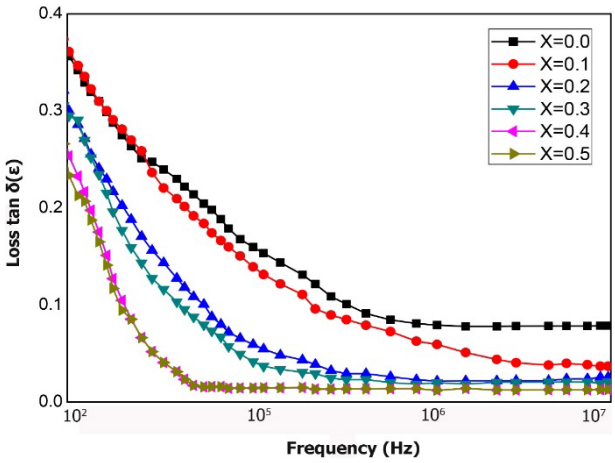

Fig. 5. Tangent loss.

The Figure 5 shows the tangent loss difference for the corresponding temperature. Whenever the polarization delays while beyond applied field, dielectric loss occurs, which is produced by grain boundary phenomenon, contaminant, and crystal defects. The density is also one of the factors for tangent loss. Large porosity specimens get a low density, resulting in a lower dielectric constant and excessive losses. The significant number of correlation is to the high electrical conductivity owing to the grain boundary at low frequencies. As a consequence, an electron hopping requires more energy, resulting in significant energy loss. However, during higher frequencies, a tiny effort is necessary, resulting in low impedance and minimal power losses.

3.3. Magnetic properties

At room temperature, EPR spectra of $Co_{0.5}Zn_{0.5}Cd_xFe_{(2-x)}O_4$ (x-0.0, 0.1, 0.2, 0.3, 0.4, and 0.5) nanocomposites were recorded and shown in Fig 6. The Lorentzian distribution function was used to calculate the $\Delta H_{PP}(line\ width)$, g-value, and spin concentration from the spectra. The existence of isolated Fe^{3+}, Cd^{2+}, and Zn^{2+} ions is indicated by the presence of a single resonance wide signal with a very low convex signal of g-value of 4.2 in EPR spectra. The EPR signal's unique diverse is accounted for the different orientations of magnetic nanoparticles in low Cd concentration samples, which dispersion in the directions of the nanoparticles' anisotropic field.

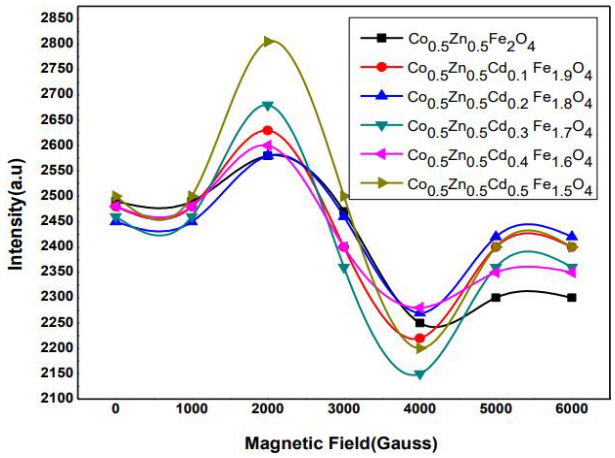

Fig. 6. EPR spectra of $Co_{0.5}Zn_{0.5}Cd_xFe_{(2-x)}O_4$.

Fig 7 shows hysteresis loops drawn from these measurements, and Table 6 shows the saturation magnetization (Ms), ramanence magnetization (Mr), and coercitivity (Hc) values derived from all these loops (Kaur et al 2019). The reduction in apex cut-off wavelength in the $Co_{0.5}Zn_{0.5}Cd_xFe_{(2-x)}O_4$ sample can be attributed to the isotropic orientation of magnetization as cadmium concentration increased. The search coil approach was used to assess DC magnetization.

At ambient temperature, the magnetism characteristics of the synthesized samples were investigated using a vibrating sample magnetometer (VSM) with an applied tensile field of 10000Oe. The hysteresis loop of Co-Zn ferrites $Co_{0.5}Zn_{0.5}Fe_2O_4$ and $Co_{0.5}Zn_{0.5}Cd_{0.5}Fe_{1.5}O_4$ which are ensure the ferromagnetic behavior of prepared samples at 1000^0C. Based on the study of all of these hysteresis loops, it is possible to conclude that the ferromagnetic behavior of the materials has been modified by the doping of non-magnetic Zn and Cd ions to replace magnetic cobalt ions. As shown in Table 1, the magnetic properties of produced samples, such as Remanence magnetization (MR), coercivity (Hc), and squareness ratio (MR/MS), diminish with Zn and Cd ion doping. Although moderate saturation magnetization (Ms) can be achieved by doping Zn and Cd ions into cobalt ferrite large importance is required for high-frequency passive components in permanent magnets.

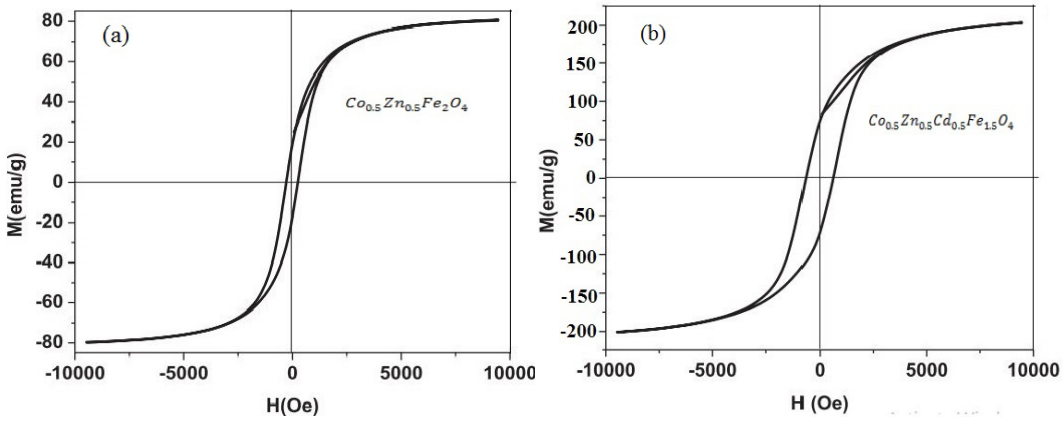

Fig. 7. Magnetic hysteresis loops (a) $Co_{0.5}Zn_{0.5}Fe_2O_4$ (b) $Co_{0.5}Zn_{0.5}Cd_{0.5}Fe_{1.5}O_4$.

Table 1. Magnetization parameters.

Sample	M_s	M_r	H_c
	emu/gm	emu/gm	Oe
$Co_{0.5}Zn_{0.5}Fe_2O_4$	121.86	13.52	280.43
$Co_{0.5}Zn_{0.5}Cd_{0.1}Fe_{1.9}O_4$	142.74	22.45	334.65
$Co_{0.5}Zn_{0.5}Cd_{0.2}Fe_{1.8}O_4$	156.32	25.71	445.64
$Co_{0.5}Zn_{0.5}Cd_{0.3}Fe_{1.7}O_4$	167.93	28.93	876.54
$Co_{0.5}Zn_{0.5}Cd_{0.4}Fe_{1.6}O_4$	170.54	36.52	1152.4
$Co_{0.5}Zn_{0.5}Cd_{0.5}Fe_{1.5}O_4$	194.61	42.65	1380.3

Fig 7 shows the magnetic hysteresis loops of various synthesized copper ferrites. Cobalt ferrite enriched containing zinc ion, on the other hand, has a shorter loop than soft ferrite. The saturation magnetization values of produced samples range from 121.86 emu/g to 194.61 emu/g, as shown in Table 1. Furthermore, the saturation magnetization (Ms) of cobalt ferrite is 121.86 emu/g, which is consistent with the previously reported results (Kaur et al 2019). Furthermore, Zn^{2+} and Cd^{2+} occupy the A-site, MS values rise when they are doped. Dopants have shifted Fe^{3+} to the B-site, increasing magnetization; however, the magnetic moment of the A-site is decreasing due to a rise in non-magnetic

Zn^{2+} ions in the A-site. As a result, the concentration of Fe2+ ions in the B-site rises. As a result, the A-B attraction among magnetic ions weakens, increasing the overall magnetization values Ms even more.

The addition of Cd^{2+} doping in cobalt ferrite has exhibited the very same behavior. The increase in M_s caused by Zn^{2+} and Cd^{2+} doping is in good agreement with other researchers' previously published experiment results (Somaiah et al 2012). The coercivity (Hc) values are ranged from 280.4 Oe to 1380.3 Oe due to the anisotropic morphology of spinel ferrites and non-magnetic Zn^{2+} ions. Therefore, in the case of cobalt zinc ferrite the Hc value is less than 280.4 Oe. Because of the gradual increase in crystallinity and particle size, the value of saturation magnetization in cadmium doped Co-Zn ferrites increased from 142.74 emu/ g to 194.61 emu/g as the temperature increased. The MR value ranges from 13.52 emu/ g to 42.65 emu/g, however in the case of zinc doping, the MR value is much lower, and therefore we obtained a soft ferrite sample of $Co_{0.5}Zn_{0.5}Fe_2O_4$, which could be because zinc is a non-magnetic intrinsic structure.

4. Conclusion

Cadmium doped Zn ferrites $Co_{0.5}Zn_{0.5}Cd_xFe_{(2-x)}O_4$ (x-0.0, 0.1, 0.2, 0.3, 0.4, and 0.5) were synthesized by coprecipitation method and spinel ferrite structure was confirmed by previous experimental studies. The addition of Cd remarkably improves the dielectric properties of the and tangent loss of the prepared material. From the graphical observation of the actual part of the dielectric constant formed in the range 2 to 8, the imaginary region of the dielectric constant at different concentrations of cadmium ions from 0.002 to 0.0045 was detected. The ac conductivity value was found as $4.2X10^{-7}$ S/cm for $Co_{0.5}Zn_{0.5}Cd_{0.5}Fe_{1.5}O_4$ ferrofluids. The cadmium added Co-Zn ferrites of saturation magnetization raises from 142.74 emu/ g to 194.61 emu/g, as well as temperature increases. MR value rages from 13.52 emu/g to 42.65 amu/g. Furthermore, the coercive fields (Hc) are moderate and Hc, and the crystal size of the $Co_{0.5}Zn_{0.5}Cd_xFe_{(2-x)}O_4$magnetic particles contribute to the super-paramagnetic behavior at ambient temperature, while the $Co_{0.5}Zn_{0.5}Cd_xFe_{(2-x)}O_4$ magnetic nanoparticles are the precursor to the super paramagnet.

Acknowledgements

The author Dr.S.Sendhilnathan, gratefully acknowledges the Department of science and Technology (Ref.No.SR/FTP/PS-59/2008) for the financial assistance received throughout the project.

References

[1] L. Filipponi, D. Sutherland, Nanotechnology - A Brief Introduction (2007).

[2] Rosensweig RE. Ferro hydrodynamics. London: Cambridge University Press; 1985.

[3] Hiegeister R, Andra W, Buske N, Hergt R, Hilger I, Richter U, Kaiser W., J Magn Magn Mater 1999; 201:420-2; https://doi.org/10.1016/S0304-8853(99)00145-6

[4] Nakatsuka K, Jeyadevan B, Neveu S, Koganezawa H., J Magn Mater 2002; 252:360-2; https://doi.org/10.1016/S0304-8853(02)00683-2

[5] Shuchi S, Sakatani K, Yamaguchi H., J Magn Mater 2005; 289:257-9; https://doi.org/10.1016/j.jmmm.2004.11.073

[6] S.B. Somvanshi, et al., AIP Conference Proceedings., AIP Publishing, 2019; https://doi.org/10.1063/1.5113361

[7] S.B. Somvanshi, et al., Ceram. Int. 46 (2019); https://doi.org/10.1016/j.ceramint.2019.11.265

8. S.R. Patade, et al., Nanomater. Energy (2020) 1-7; https://doi.org/10.1680/jnaen.19.00006

[9] S.B. Kale, et al., AIP Conference Proceedings, AIP Publishing LLC, 2018; https://doi.org/10.1063/1.5032528

[10] S. Alone, et al., J. Alloys Compd. 509 (16) (2011) 5055-5060; https://doi.org/10.1016/j.jallcom.2011.02.006

[11] P.B. Kharat, et al., AIP Conference Proceedings., AIP Publishing LLC, 2018; https://doi.org/10.1063/1.5028675

[12] P.B. Kharat, et al., J. Mater. Sci. Mater. Electron. 30 (7) (2019) 6564-6574; https://doi.org/10.1007/s10854-019-00963-4

[13] S. Rohilla, S. Kumar, P. Aghamkar, S. Sunder, A. Agarwal, J. Magn. Magn. Mater. 323 (2011) 897-902; https://doi.org/10.1016/j.jmmm.2010.11.001

[14] A. Tomitaka, T. Koshi, S. Hatsugai, T. Yamada, Y. Takemura, J. Magn. Magn. Mater. 323 (2011) 1398-1403; https://doi.org/10.1016/j.jmmm.2010.11.054

[15] Z. Ghasemian, D.S. Gahrouei, S. Manouchehri, Avicenna J. Med. Biotechnology. 7 (2) (2015) 64-68.

[16] M. Rahimi, et al., J. Magn. Magn Mater. 347 (2013) 139-145; https://doi.org/10.1016/j.jmmm.2013.08.004

[17] S. Munjal, et al., J. Magn. Magn Mater. 404 (2016) 166-169; https://doi.org/10.1016/j.jmmm.2015.12.017

[18] A. Raut, et al., J. Magn. Magn Mater. 358 (2014) 87-92; https://doi.org/10.1016/j.jmmm.2014.01.039

[19] P. Coppola, et al., J. Nanoparticle Res. 18 (5) (2016) 138; https://doi.org/10.1007/s11051-016-3430-1

[20] M. Hossain, Study of the Magnetic and Transport Properties of Ytterbium Doped Co-Zn Ferrites, Khulna University of Engineering & Technology (KUET), Khulna, Bangladesh, 2018.

[21] R.K. Sharma, O. Suwalka, N. Lakshmi, K. Venugopala, A. Banerjee, P.A. Joy, Mater. Lett. 59 (2005) 3402-3405; https://doi.org/10.1016/j.matlet.2005.06.004

[22] G. Sathishkumar, C. Venkataraju, K. Sivakumar, Mater. Sci. Appl. 1 (2010) 19-24; https://doi.org/10.4236/msa.2010.11004

[23] G. Raju, N. Murali, M.S.N.A. Prasad, B. Suresh, B. Kishore Babu, Mater. Sci. Energy Technol. 2 (1) (2019) 78-82; https://doi.org/10.1016/j.mset.2018.11.001

[24] A.B. Kulkarni, S.N. Mathad, Int. J. Self Propag. High Temp. Synth. 27 (1) (2018) 37-43; https://doi.org/10.3103/S106138621801003X